

Tailored polymer coatings as corrosion inhibitor for mild steel in acid medium

Ghada M. Abd El-Hafeez, Mohamed M. El-Rabeie, Ahlam F. Gaber & Zeinab R. Farag

Journal of Coatings Technology and Research

ISSN 1547-0091

Volume 18

Number 2

J Coat Technol Res (2021) 18:581-590

DOI 10.1007/s11998-020-00426-0

Your article is protected by copyright and all rights are held exclusively by American Coatings Association. This e-offprint is for personal use only and shall not be self-archived in electronic repositories. If you wish to self-archive your article, please use the accepted manuscript version for posting on your own website. You may further deposit the accepted manuscript version in any repository, provided it is only made publicly available 12 months after official publication or later and provided acknowledgement is given to the original source of publication and a link is inserted to the published article on Springer's website. The link must be accompanied by the following text: "The final publication is available at link.springer.com".



Tailored polymer coatings as corrosion inhibitor for mild steel in acid medium

Ghada M. Abd El-Hafeez, Mohamed M. El-Rabeie, Ahlam F. Gaber, Zeinab R. Farag 

Received: 6 May 2020 / Revised: 10 September 2020 / Accepted: 21 September 2020
© American Coatings Association 2021

Abstract Poly(*o*-bromophenol-co-*N*-methylaniline) [poly(OBP-co-NMA)] was electropolymerized in an acidic medium at 30°C under inert atmosphere. The formed polymer was characterized using IR spectroscopy, XRD, SEM and TGA analysis. The efficiency of the deposited polymer as a corrosion protection coating on a mild steel electrode in an acidic medium was investigated. Corrosion and impedance measurements reveal that the prepared polymer has excellent passivation properties. The free energy of adsorption of the prepared polymer on the electrode surface was in the range of ≈ -19.5 kJ mol⁻¹, which reveals a physical adsorption of the inhibitor molecules on the metallic surface.

Keywords Electropolymerization, Mild steel, Corrosion inhibition, Cyclic voltammograms, Coatings

Introduction

Conducting polymers have a wide range of technological applications such as rechargeable batteries, sensors and electronics.^{1–7} Organic polymers have been established as organic corrosion inhibitors, and they are easily adsorbed onto the metal surface forming a barrier coating layer which reduces active corrosion sites. Also, they provide a potential cheap alternative to chromium and phosphate treatments and their associated pollution.⁸ Previous studies indicated that organic compounds containing –NH₂ and/or –OH groups retard the corrosion reaction due to the formation of a protective surface layer or by prevent-

ing oxidation. One of the well-known conducting polymers which are mentioned because of their inhibition features is polyaniline (PANI) due to its high electrical conductivity, low cost and anticorrosivity.^{9–12} Polyphenols were also investigated as corrosion inhibitors.^{13–16} The potential-time diagrams of the electropolymerization of aniline on carbon steel is composed of three steps: the dissolution and formation of polycrystalline interphase, passivation and electropolymerization.^{17,18} Polyaniline derivatives and polyaniline copolymers have been synthesized and applied as corrosion inhibitors.^{14,19} Due to its industrial importance, applications in construction and its excellent mechanical properties, corrosion on mild steel receives significant consideration. So, corrosion protection of mild steel is of great economic importance.²⁰ Among the corrosion inhibitors which can be used are polymers.^{14,19,21} Polymers could be synthesized easily and have a good surface coverage when deposited “coated.” Recently, poly(*N*-2-hydroxyethylaniline-co-2-chloroaniline) has been used as an inhibitor for mild steel in acid medium.²² Khalaf et al. studied the corrosion protection of mild steel in acidic medium by coating it with TiO₂ thin films co-doped with NiO and ZrO₂ in acidic chloride environments.²³ Cationic surfactants such as cationic gemini surfactants and peptidomimetic cationic surfactants were also studied.^{24,25} Salicylaldehyde azine-functionalized polybenzoxazine nanocomposites and spirocyclopropane derivatives have been used for inhibiting the mild steel corrosion.^{26,27}

Conducting polymeric inhibitors (CP) were recently used due to their industrial applications and economic viability. Upon adsorption of these polymers they prohibit large areas of the metal surface. On the other hand, polymers act as excellent inhibitors when used in low concentrations when compared with simple organic ones. The efficiency of these inhibitors depends on their ability to be adsorbed on the metal medium

G. M. Abd El-Hafeez, M. M. El-Rabeie,
A. F. Gaber, Z. R. Farag (✉)
Chemistry Department, Faculty of Science, Fayoum
University, 63514 Fayoum, Egypt
e-mail: zrf00@fayoum.edu.eg

interface and the covered surface area by the inhibitor. Also, the high molecular weight and the large molecular size of the inhibitor ensure the greater coverage of the metallic surface which lead to higher inhibition efficiency.²⁸

In the present work poly(*o*-bromophenol-co-*N*-methylaniline) [poly(OBP-co-NMA)] was electrodeposited, characterized and then applied as corrosion inhibitor for mild steel in an acidic medium.

Materials and experimental procedures

Materials and solutions

O-bromophenol and *N*-methylaniline were obtained from Merck Schuchardt (Germany), and sulfuric acid, ethanol and acetone were provided by El-Nasr Pharmaceutical Chemical Company (Egypt). The chemicals used are of analytical grade and were used as received. All solutions were prepared using freshly double-distilled water under N₂ gas and were prepared in the electrochemistry laboratory at the Faculty of Science, Fayoum University.

Electrochemical measurements

A three-electrode system was used to evaluate the electrochemical performance of the mild steel electrode in a naturally aerated stagnant acidic solution (pH = 2) prepared from 1 M H₂SO₄ aqueous solution. Before all electrochemical measurements, the working electrode was left for at least 1 h. All electrochemical measurements were taken with the help of a Volta lab potentiostat (Radiometer PGZ301). A saturated calomel electrode SCE and a platinum electrode were used as the reference and counter electrodes, respectively. The working electrode was made of a mild steel rod obtained by an up-casting procedure. It was prepared in a metallurgical workshop. The metallic rod was introduced into glass tubes using a two-component epoxy resin leaving a surface area of 0.5 cm² to contact the solution. The chemical composition of the pure carbon steel is listed in Table 1. Electrochemical impedance spectroscopy (EIS) was performed at a steady-state potential. EIS was performed within the frequency range of 100 000–0.05 Hz with a peak to peak amplitude of 5 mV.^{29,30} Electrochemical impedance parameters have been fitted using the *Z_m* view software with a suitable equivalent circuit. Potentio-

dynamic polarization measurements were executed over the sweeping potential range of 500 to 60 mV at a scan rate of 10 mV s⁻¹. Before every measurement, the mild steel electrode was polished by consecutive emery papers ranging from 600 to 2500 grit and was then carefully washed with bi-distilled water and dried using a soft paper. Subsequently, direct dipping in the corrosive medium was done. To obtain the desired concentration from the as-prepared polymer, a certain amount of polymer was dissolved into the acidic solution (pH = 2) samples. A series of solutions with lower concentrations were prepared by dilution. To verify the reproducibility, every experiment was repeated at least three times.

Preparation of poly(OBP-co-NMA)

Electropolymerization of poly(OBP-co-NMA) from aqueous solution containing 0.060 mol L⁻¹ of monomer, 0.2 mol L⁻¹ H₂SO₄ at 30°C was performed with scan rate of 40 mV s⁻¹.

The working electrode was a platinum foil with dimensions of 1 cm length and 0.5 cm width containing a platinum wire (0.75 cm) to facilitate the electrical connection. Before each run, the platinum electrode was cleaned and washed with ethanol, double-distilled water and dried.

The polymer solution used for corrosion measurements was prepared by weighing 0.1 g from polymer, with drops of ethanol to dissolve the polymer followed by addition of 100 ml acidic buffer [pH = 2]. From the prepared solution (5 ml, 7.5 ml and 10 ml) were taken and completed to 100 ml acidic buffer. The electrical cell in which a platinum wire auxiliary electrode acts as a cathode and the mild steel working electrode acts as an anode was used for measurements, and it was followed over 1 h in a stagnant naturally aerated aqueous solution of pH = 2. At the end of each experiment, the working electrode was picked up, washed and dried for corrosion measurement.^{14,31}

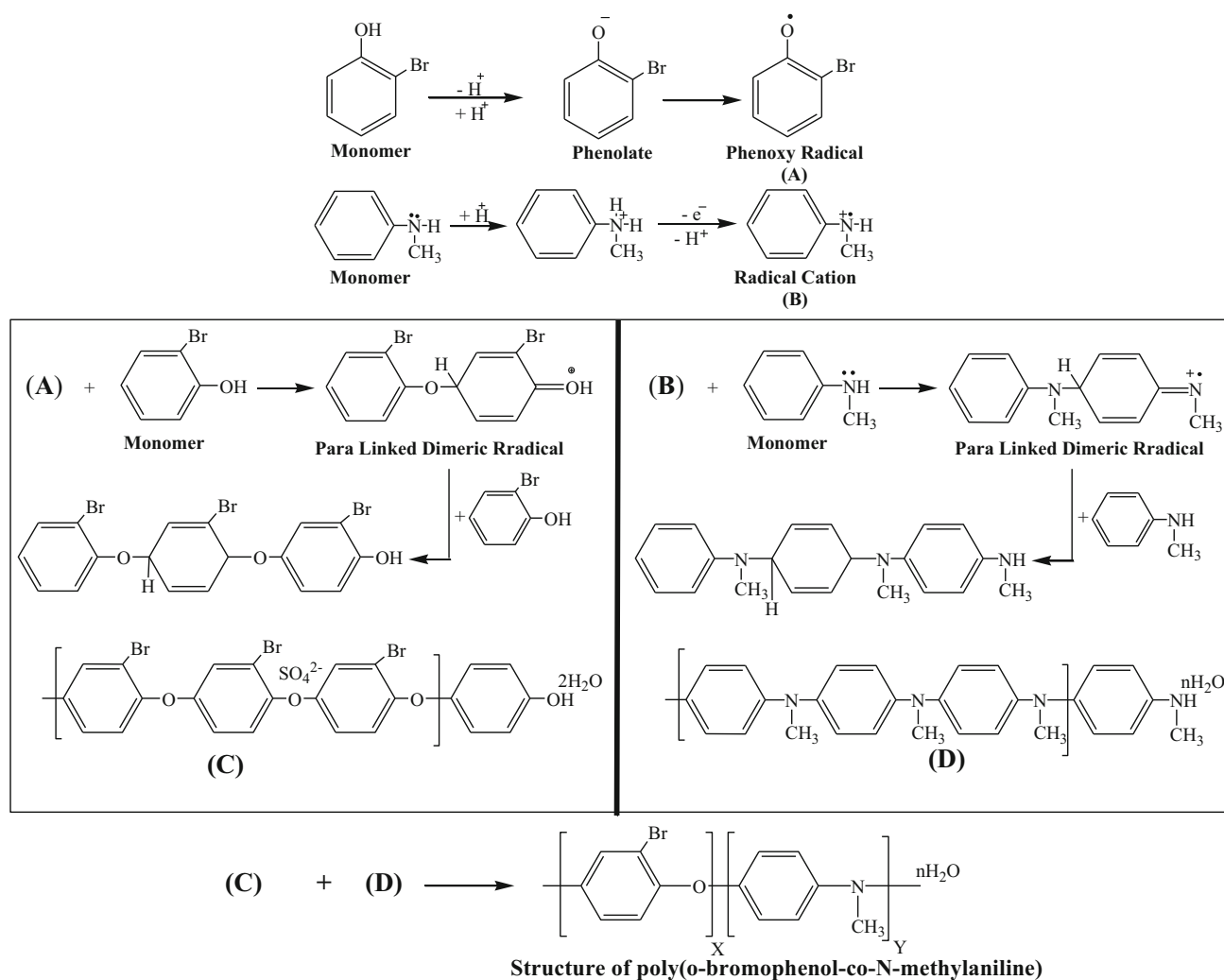
Characterization of the electrodeposited polymer

Infrared, UV-visible and ¹HNMR spectroscopy

Ultraviolet spectroscopy was carried out using SHIMADZU UV Spectrophotometer (M160 PC) at room temperature in the range 200–400 nm using ethyl alcohol as a solvent and reference. IR measurements were taken using a SHIMADZU FTIR-340 Jasco Spec-

Table 1: Chemical composition (wt%) of the mild steel electrode

Element	C	Si	Mn	S	P	Cu	Cr	Ni	Al	Fe
Analysis	0.34	0.26	0.93	0.02	0.04	0.01	0.01	0.02	0.01	Balance



Scheme 1: Polymerization mechanism

trophotometer (Japan), and the KBr pellets disk technique was used. Dimethylsulfoxide (DMSO) was used for $^1\text{H-NMR}$ measurements which were performed using a Varian EM 360L, 60-MHz NMR spectrometer.

Thermogravimetric analysis (TGA)

Thermogravimetric analysis (TGA) using a SHIMADZU DT-30 thermal analyzer (SHIMADZU, Kyoto, Japan) was performed. The measurements were recorded from room temperature up to 600°C , at the rate of $20^\circ\text{C}/\text{min}$ and nitrogen $50\text{ cm}^3/\text{min}$.

Electron microscope and XRD

Scanning electron microscopy (SEM) analysis was carried out on the polymer film deposited on the Pt-working electrode surface using a JSM-T20 Electron

Probe Micro Analyzer (JEOL, Tokyo, Japan). The X-ray diffraction analysis (XRD) (Philips 1976 Model 1390, Netherlands) was operated using Cu X-ray tube, Scan speed: $8\text{ deg}/\text{min}$, current 30 mA, voltage 40 kV and 10 s preset time.

Results and discussion

Characterization of the electrodeposited polymers

Elemental analysis

The elemental analysis data were not useful due to the different possibilities of copolymer structure. The structure of the obtained copolymer was confirmed using UV–visible, IR, $^1\text{H-NMR}$, TGA, XRD and SEM. A proposed polymerization mechanism and the structure of the copolymer are represented in Scheme 1.

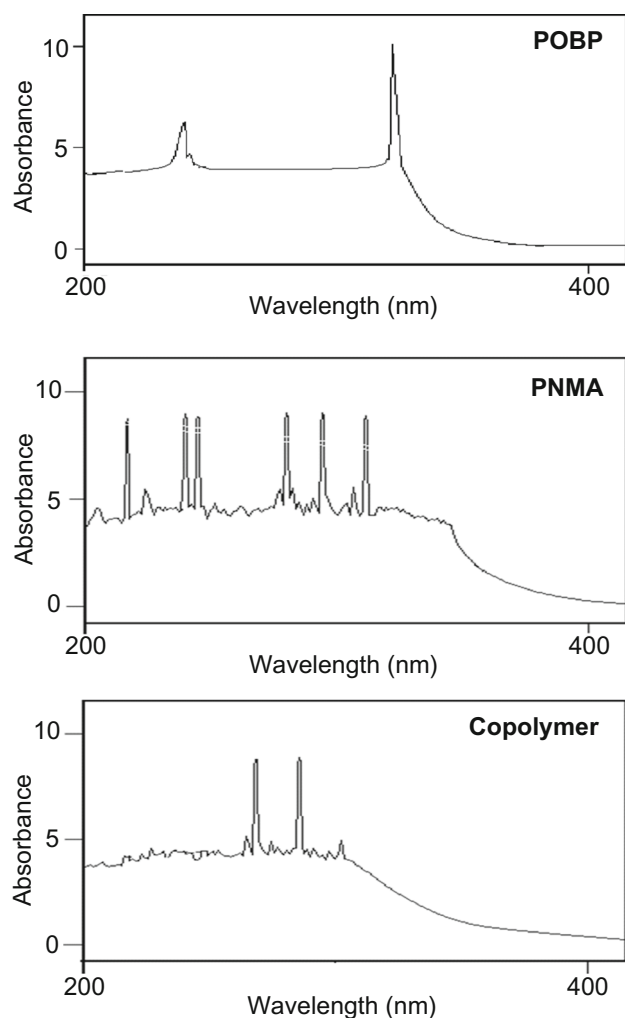


Fig. 1: UV-visible assignments of POBP, PNMA and poly(OBP-co-NMA)

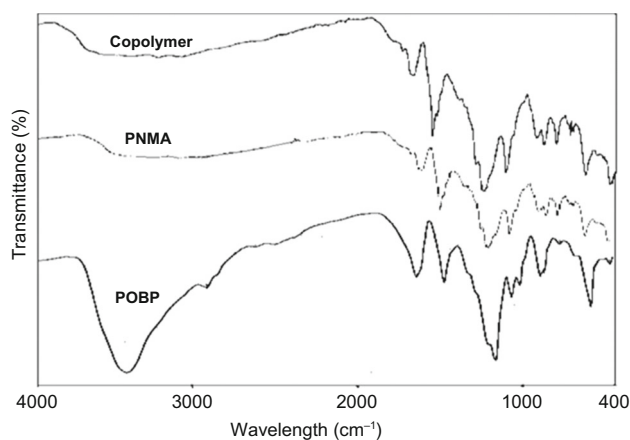


Fig. 2: Infrared spectra of POBP and PNMA and poly(OBP-co-NMA)

The ultraviolet-visible spectra

The UV-visible spectra of poly(*o*-bromophenol) (POBP), poly(*N*-methylaniline) (PNMA) and poly(*o*-bromophenol-co-*N*-methylaniline) [poly(OBP-co-NMA)] are represented in Fig. 1.

1. In the case of POBP, three absorption bands appear at $\lambda_{\max} = 210, 306$ and 329 nm which may be attributed to (E_2 -band) transition of the benzene ring and β -band ($A_{1g}-B_{2u}$), respectively.
2. In the case of PNMA, absorption bands appear from $\lambda_{\max} = 220, 243, 253, 290, 310$ and $\lambda_{\max} = 325$ nm which may be attributed to the transition (E_2 -band) of the benzene ring and β -band ($A_{1g}-B_{2u}$), respectively.
3. In the case of poly(OBP-co-NMA), three absorption bands appear at $\lambda_{\max} = 280, 290$ and 310 nm which may be due to the high conjugation of the aromatic polymeric chains.

Infrared spectroscopy

The infrared spectra of POBP, PNMA and poly(OBP-co-NMA) are represented in Fig. 2. The infrared absorption bands are illustrated in Table 2.

^1H NMR spectroscopic measurements

The ^1H NMR spectrum of POBP, PNMA and poly(OBP-co-NMA) are represented in Fig. 3. The figure shows one solvent signal at $\delta = 2.51$ ppm. The protons of benzene rings in the polymeric structure appear in the region from $\delta = 6.20$ to $\delta = 8.23$ ppm. A singlet signal at $\delta = 2.40$ ppm which may be attributed to protons of CH_3 group. The signals of different OH disappeared when deuterated water was used.

Thermogravimetric analysis

TGA for the electrochemically prepared polymer samples was investigated, and the TGA-curve is represented in Fig. 4. The diagram shows three stages during the thermolysis of the prepared polymer samples. The first stage includes the loss of water molecules in the temperature range between 35.37 and 54.63°C , and the weight loss was found to be (2.91%).

In the second stage, the bonded water molecules are thermally decomposed in the range of 150 to 200°C . The weight loss was found to be (5.75%) in the temperature range between 55.11 and 126.5°C .

The third stage is the decomposition of the dopants present in the polymer structure adding to the decom-

Table 2: Infrared absorption bands of POBP, PNMA and poly(OBP-co-NMA)

Assignments	Wavenumber (cm ⁻¹)		
	POBP	PNMA	Copolymer
CH out of plane bending for 1,2 di-substituted benzene ring	749 ^s	665 ^m	751 ^w
	826 ^m	815 ^m	824 ^b
Stretching vibration for C–Br group	934 ^w	1035 ^w	–
Stretching vibration for C–O group	1030 ^s	–	1043 ^m
Stretching for incorporation in the polymer sulfate group	1189 ^s	–	1177 ^w
Stretching vibration of C=C in benzene ring	1475 ^s	–	1469 ^m
	1588 ^s	1619 ^w	1585 ^m
	1777 ^w	–	–
Stretching vibration for CH aromatic	3069 ^w	–	3064 ^b
Stretching vibration intermolecular hydrogen solvated OH group or end group OH of polymeric chain	3499 ^b	3226 ^b	–

s strong; w weak; b broad; m medium

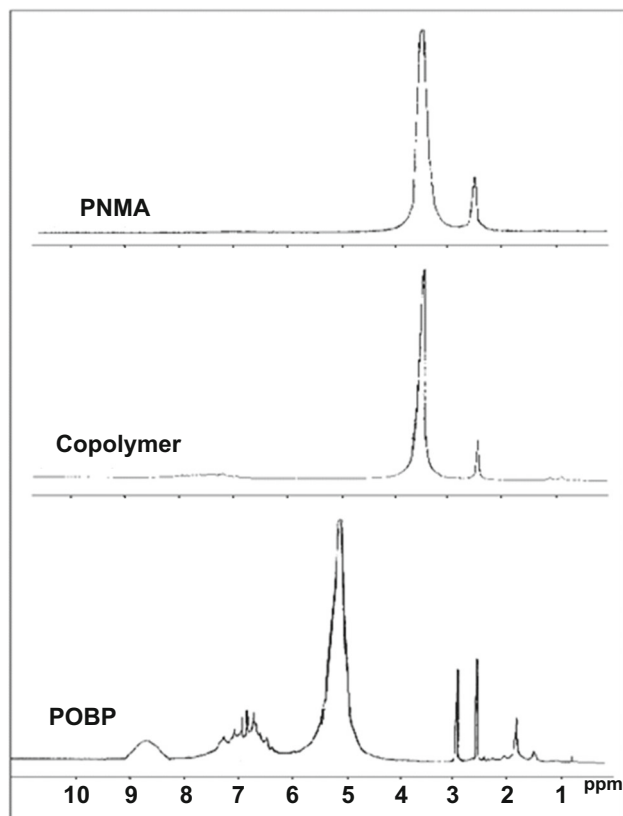


Fig. 3: ¹H NMR spectra of POBP, PNMA and poly(OBP-co-NMA)

position of the remaining part of the polymer which started at about 180 to 350°C. The weight loss in the range of temperature between 127.5 and 599.3°C was found to be (88.4%) which includes the decomposition of the remaining part of the polymer in the range from 385–600°C.

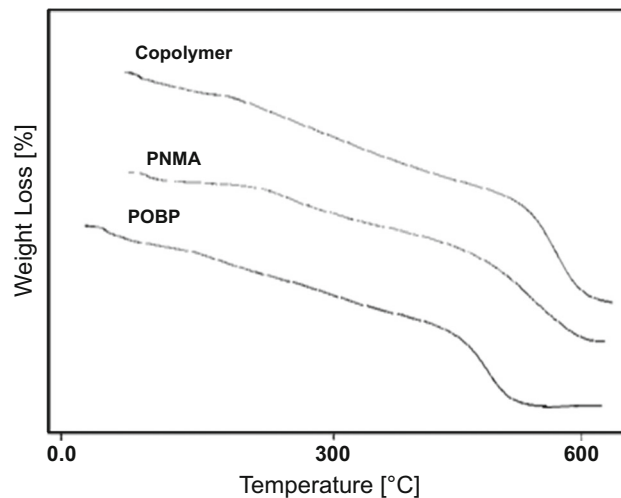


Fig. 4: Thermogravimetric analysis of POBP, PNMA and poly(OBP-co-NMA)

Surface morphology and x-ray diffraction

Under most conditions, the electrodeposited copolymer film of poly(OBP-co-NMA) on the platinum electrode surface at the optimum conditions was brown, homogeneous, smooth and well-adhering to the electrode surface. The surface morphology of the deposited copolymer film was examined using SEM (Fig. 5a) and XRD (Fig. 5b).

Application of poly(OBP-co-NMA) as corrosion inhibitor for mild steel in acidic medium (pH = 2)

Open circuit potential measurements

Open circuit potential of mild steel in the presence of different concentrations of poly(OBP-co-NMA), namely 0, 20 ppm, 50 ppm and 100 ppm, was followed

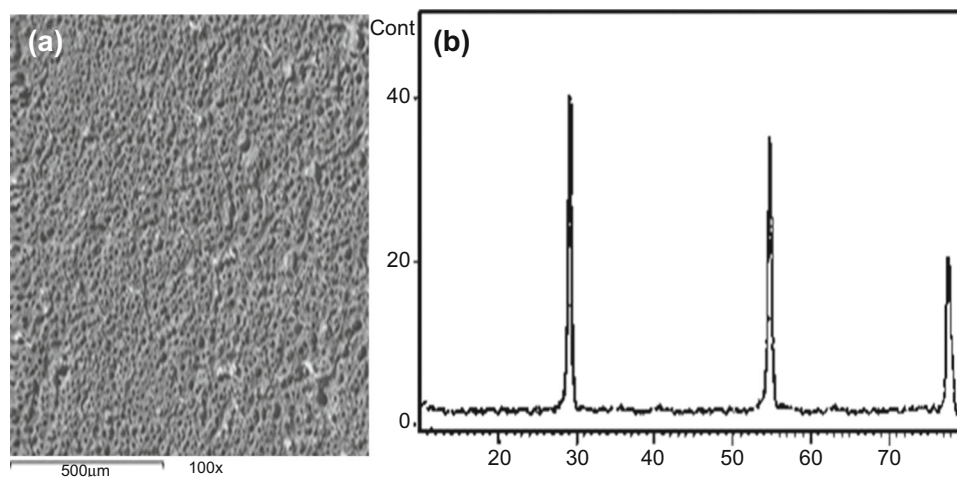


Fig. 5: (a) Scanning electron microscope (SEM) and (b) X-ray diffraction (XRD) of poly(OBP-co-NMA)

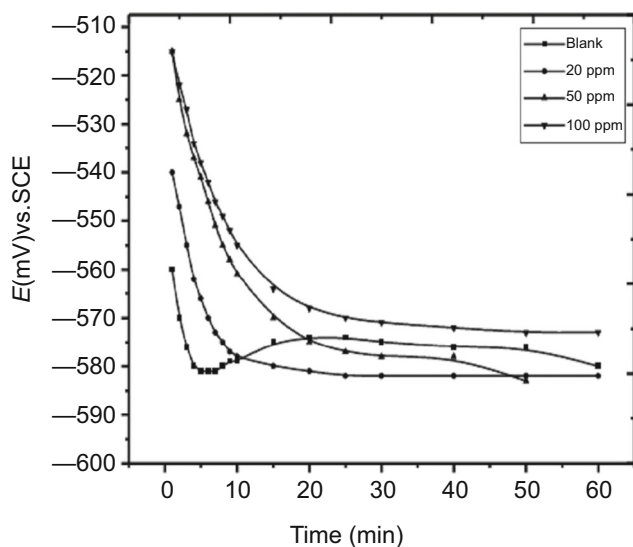


Fig. 6: Variation of the open circuit potential of mild steel alloy with time in stagnant naturally aerated aqueous solutions of pH = 2 in the presence different concentrations of poly(OBP-co-NMA) at 25°C

over 1 h in stagnant naturally aerated aqueous solution of pH = 2 (1 M H₂SO₄). The results show that the presence of polymer shifts the steady-state potentials to more negative values. The result is presented in Fig. 6.

Potentiodynamic polarization (the Tafel extrapolation) technique

The electrochemical behavior of mild steel in different concentrations of poly(OBP-co-NMA) (blank, 20 ppm, 50 ppm, 100 ppm) in a naturally aerated aqueous solution of pH = 2 was investigated under polarization conditions, and the linear polarization and Tafel

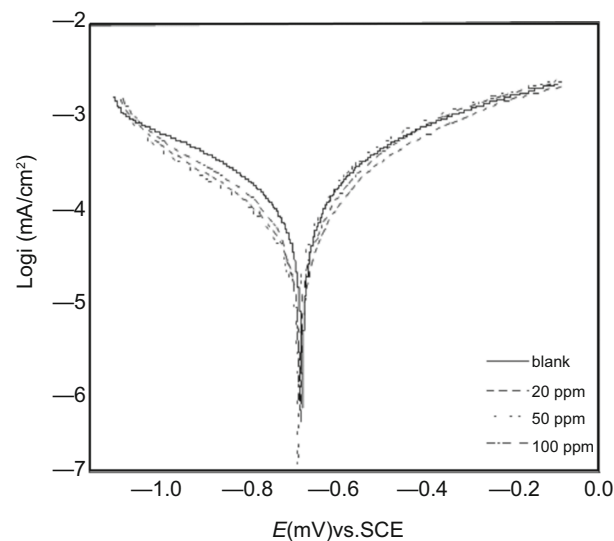


Fig. 7: Potentiodynamic polarization curves of mild steel alloy in stagnant naturally aerated aqueous solutions of pH = 2 in the absence and presence of poly(OBP-co-NMA) at 25°C

extrapolation techniques were carried out at a scan rate of 10 mV s⁻¹.

Figure 7 illustrates the potentiodynamic polarization curves of different concentrations of copolymer after holding the mild steel electrode at the open circuit potential for 1 h in a naturally aerated aqueous solution of pH = 2.

The figure shows that the corrosion potential shifted to a negative direction, the presence of different copolymer concentrations with decreasing anodic and cathodic current densities indicating that poly(OBP-co-NMA) acts as a mixed inhibitor, i.e., the prepared copolymer adsorbed on both anodic and cathodic active sites on the metal surface, blocking the active sites for the corrosion process, thus decreasing the exposed free metal area to the corrosive medium.

Table 3: Potentiodynamic polarization parameter of mild steel after 1 h of electrode immersion in stagnant naturally aerated polymer solution in naturally aerated aqueous acidic solution pH = 2 at 25°C

Copolymer concentration	E_{corr} (mV)	R_p ($k\Omega \text{ cm}^{-2}$)	i_{corr} ($\mu\text{A cm}^{-2}$)	β_a (mV)	β_b (mV)	Corrosion rate ($\mu\text{m y}^{-1}$)	$\eta\%$
Blank	- 670.6	0.502	107.1	263.4	- 345.1	1.33	0
20 ppm	- 675.7	0.872	70.6	254.9	- 359.5	0.88	34.1
50 ppm	- 679.5	1.02	65.4	227.4	- 366.6	0.81	38.9
100 ppm	- 688.8	1.05	48.6	212.3	- 292.6	0.61	54.6

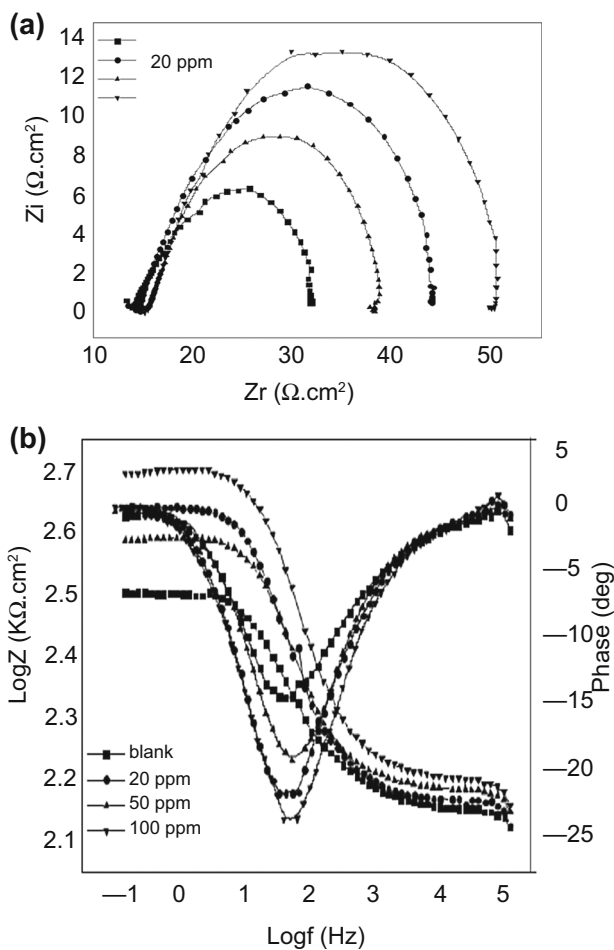


Fig. 8: (a) Nyquist plot and (b) Bode plot of mild steel alloy in stagnant naturally aerated aqueous solutions of pH = 2 in the presence of poly(OBP-co-NMA) at 25°C

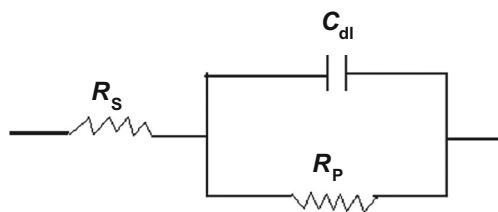


Fig. 9: Equivalent circuit model for a simple electrochemical cell (Randles Model)

The results of corrosion parameters, Tafel slopes (β_a and β_b), corrosion potential (E_{corr}), corrosion current density (i_{corr}), corrosion rate and the corrosion protection efficiency ($\eta\%$)³² of the copolymer coat film were calculated and are presented in Table 3.

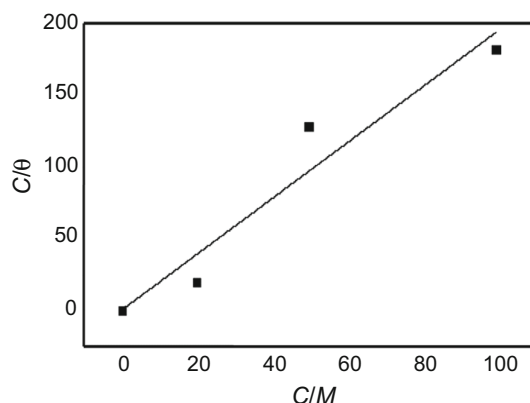
Table 3 shows that the Tafel slopes (β_a and β_b) are in most cases increased with increasing polymer concentration which indicates that the corrosion process is under activation control, and the corrosion current density i_{corr} and the corrosion rate decreases with an increase in the polymer concentrations; this indicates that the copolymer has better corrosion resistance. The inhibition of mild steel alloy by the prepared copolymer could be attributed to the adsorption of these molecules onto the electrode surface. This is made possible due to the presence of heteroatoms of nitrogen, oxygen and even π electrons, which are regarded as adsorption centers. The functional groups ($-\text{NH}_2$, $-\text{C}=\text{O}$) in this copolymer could be bridged between the polymer and the surface of the metal.²⁹

Electrochemical impedance measurements

The electrochemical impedance investigations of mild steel alloy in a naturally aerated acidic solution pH = 2 in the absence and presence of different concentrations of the prepared poly(OBP-co-NMA) are shown as Bode plots in Figs. 8a and 8b. The figures show one phase maximum at the intermediate frequency, the broadening of phase maximum increase with increasing concentration of the prepared copolymer indicating the presence of a protective layer on the electrode surface. The response of the system in the Nyquist complex plane in Fig. 8a consists of one semicircle. The time constant or diameter of the semicircle increases with the increase in copolymer concentration. The simple equivalent circuit model (Randles equivalent circuit) with a constant-phase element (CPE) was introduced to analyze the impedance data arising from a linear range of experimental system corresponding to a simple charge-transfer process, as shown in Fig. 9. The impedance parameters of the investigated polymer were calculated and are presented in Table 4. The results of these experiments show that the film resistance has its maximum value in the presence of poly(OBP-co-NMA) at a concentration of 100 ppm. This result is in good agreement with the results of the

Table 4: Equivalent circuit parameters for steel recorded after 1 h of electrode immersion in stagnant naturally aerated polymer solution at steady-state potential at 25°C

Copolymer concentration	$R_s/\Omega \text{ cm}^2$	$R_p/k\Omega \text{ cm}^2$	$Cdl/\mu\text{F cm}^{-2}$	α
Blank	143.1	0.183	34.8	0.997
20 ppm	151.2	0.293	27.1	0.999
50 ppm	157.7	0.236	27.0	0.998
100 ppm	161.4	0.350	18.2	0.999

**Fig. 10: Langmuir isotherm plot for the adsorption of poly(OBP-co-NMA) on mild steel alloy in stagnant naturally aerated aqueous solutions of pH = 2 at 25°C**

potentiodynamic experiments. The Cdl (the thickness of the adsorbed layer $1/Cdl$) decreases with increasing polymer concentration. From this data, poly(OBP-co-NMA) shows a good passive layer for mild steel.^{30,33,34}

Adsorption isotherm

One possible mechanism for corrosion inhibition using poly(OBP-co-NMA) is the adsorption of the inhibitor which blocks the metal surface and thus does not permit the corrosion to take place. The adsorption provides the information about the interaction among the adsorbed molecules themselves as well as their interaction with the metal surface.³⁵ In this work, the adsorption of copolymer on the mild steel electrode surface was found to obey the adsorption isotherm and is plotted in Fig. 10, where a plot of C versus C/θ yields a straight line with intercept $1/K$ as described by Langmuir adsorption isotherm. The free energy of adsorption, ΔG_{ads} , was found to be -13.49 kJ/mol . The negative values of ΔG_{ads} indicate that the adsorption process is spontaneous. The calculated value for the adsorption of poly(OBP-co-NMA) on the electrode surface is less than -40 kJ/mol , which indicates physical adsorption, i.e., there are electrostatic interactions between the charged molecules and the charged electrode and there is no chemical interaction

between the inhibitor molecules and the alloy's surface.

Conclusion

Poly(*o*-bromophenol-co-*N*-methylaniline) [poly(OBP-co-NMA)] was electropolymerized and characterized using different spectral tools. A polymerization mechanism of the electrodeposited copolymer is also suggested and confirmed. The corrosion behavior of mild steel samples coated using the cyclic voltammetry electropolymerization technique of poly(OBP-co-NMA) was studied. Different polymer concentrations up to 100 ppm were investigated as corrosion inhibitors for mild steel surface in an acidic medium of pH = 2 (1 M H_2SO_4) at 303°K. The results show that the deposited polymer films are homogeneous, have smooth lamellar surface and are of higher thermal stability. Also, the corrosion protection efficiency of the passivated mild steel samples increases with an increase in the polymer concentration, and this was confirmed by open circuit measurements which show that the presence of polymer shifts the steady-state potentials to more negative values. The potentiodynamic polarization results show that the corrosion potential was shifted to a negative direction in the presence of different copolymer concentrations with decreases in both the anodic and cathodic current density, indicating that poly(OBP-co-NMA) acts as a mixed inhibitor. A future work is in progress using the deposited polymer or depositing polymers of polyphenols-co-polyaniline derivatives and application of these polymers as anticorrosive additives.

References

- Arulepp, M, Permann, L, Leis, J, Perkson, A, Rumma, K, Jänes, A, Lust, E, "Influence of the Solvent Properties on the Characteristics of a Double Layer Capacitor." *J. Power Sources*, **133** 320–328 (2004). <https://doi.org/10.1016/j.jpowsour.2004.03.026>
- Greennan, K, Killard, AJ, Hanson, CJ, Cafolla, AA, Smyth, MR, "Optimisation and Characterisation of Biosensors Based on Polyaniline." *Talanta*, **68** 1591–1600 (2006). <http://doi.org/10.1016/j.talanta.2005.08.036>

3. Karami, H, Mousavi, MF, Shamsipur, M, "A New Design for Dry Polyaniline Rechargeable Batteries." *J. Power Sources*, **117** 255–259 (2003). [https://doi.org/10.1016/S0378-7753\(03\)0168-X](https://doi.org/10.1016/S0378-7753(03)0168-X)
4. Saxena, V, Malhotra, B, "Prospects of Conducting Polymers in Molecular Electronics." *Curr. Appl. Phys.*, **3** 293–305 (2003). [https://doi.org/10.1016/S1567-1739\(02\)00217-1](https://doi.org/10.1016/S1567-1739(02)00217-1)
5. Sengupta, PP, Barik, S, Adhikari, B, "Polyaniline as a Gas-Sensor Material." *Mater. Manuf. Process.*, **21** 263–270 (2006). <https://doi.org/10.1080/10426910500464602>
6. Wang, Y, Jing, X, "Intrinsically Conducting Polymers for Electromagnetic Interference Shielding." *Polym. Adv. Technol.*, **16** 344–351 (2005). <https://doi.org/10.1002/pat.589>
7. El-Lateef, HMABD, Elrouby, M, "Synergistic Inhibition Effect of Poly(Ethylene Glycol) and Cetyltrimethylammonium Bromide on Corrosion of Zn and Zn–Ni Alloys for Alkaline Batteries." *Trans. Nonferrous Met. Soc. China*, **30** 259–274 (2020). [https://doi.org/10.1016/S1003-6326\(19\)65197-6](https://doi.org/10.1016/S1003-6326(19)65197-6)
8. Fouda, A, Aldesoky, A, Elmorsi, M, Fayed, T, Atia, M, "New Eco-Friendly Corrosion Inhibitors Based on Phenolic Derivatives for Protection Mild Steel Corrosion." *Int. J. Electrochem. Sci.*, **8** 10219–10238 (2013)
9. El-Lateef, HMA, Khalaf, MM, "Novel Dispersed Ti₂O₃-SiO₂/Polyaniline Nanocomposites: In-Situ Polymerization, Characterization and Enforcement as a Corrosion Protective Layer for Carbon-Steel in Acidic Chloride Medium." *Colloids Surf. A Physicochem. Eng. Aspects*, **573** 95–111 (2019). <https://doi.org/10.1016/j.colsurfa.2019.04.059>
10. Li, Z, Hu, J, Li, Y, Zheng, F, Liu, J, "Self-Healing Active Anticorrosion Coatings with Polyaniline/Cerium Nitrate Hollow Microspheres." *Surf. Coat. Technol.*, **341** 64–70 (2018). <https://doi.org/10.1016/j.surfcoat.2017.11.054>
11. Tammam, RH, Fekry, AM, Saleh, MM, "Understanding Different Inhibition Actions of Surfactants for Mild Steel Corrosion in Acid Solution." *Int. J. Electrochem. Sci.*, **11** 1310–1326 (2016)
12. Wang, Y, "Preparation and Application of Polyaniline Nanofibers: An Overview." *Polym. Int.*, **67** 650–669 (2018). <https://doi.org/10.1002/pi.5562>
13. Lakshmi, D, Rajendran, S, Sathiyabama, J, "Corrosion Inhibition by Phenols—An Overview." *Int. J. Nano-Corros. Sci. Eng.*, **3** 1–18 (2016)
14. Sayyah, SM, El-Rabieci, MM, Abd El-Aafez, GM, Gaber, AF, "Electropolymerization of Ortho-Bromophenol on Pt-Electrode from Aqueous Acidic Solution; Kinetics, Mechanism, Electrochemical Studies and Characterization of the Polymer Obtained." *Int. J. Adv. Res.*, **3** 65–84 (2015)
15. Aljeaban, N, Goni, L, Alharbi, B, Mazumder, J, Ali, S, Chen, T, Quraishi, M, Al-Muallem, HJ, "Polymers Decorated with Functional Motifs for Mitigation of Steel Corrosion: An Overview." *Int. J. Polym. Sci.*, **2020** (2020). <https://doi.org/10.1155/2020/9512680>
16. Veys-Renaux, D, Reguer, S, Bellot-Gurlet, L, Mirambet, F, Rocca, EJCS, "Conversion of Steel by Polyphenolic Model Molecules: Corrosion Inhibition Mechanism by Rutin, Esculin, Esculetol." *Corros. Sci.*, **136** 1–8 (2018)
17. Li, Y, Zhang, H, Wang, X, Li, J, Wang, F, "Growth Kinetics of Oxide Films at the Polyaniline/Mild Steel Interface." *Corros. Sci.*, **53** 4044–4049 (2011). <https://doi.org/10.1016/j.corsci.2011.08.010>
18. Shinde, VP, Patil, PP, "Investigation on Role of Monomer (s) During Electrochemical Polymerization of Aniline and Its Derivatives on Low Carbon Steel by XPS." *Electrochim. Acta*, **78** 483–494 (2012). <https://doi.org/10.1016/j.electacta.2012.06.042>
19. Abd El-Salam, H, Abd El-Hafez, G, Askalany, H, Fekry, A, "A Creation of Poly (N-2-Hydroxyethylaniline-co-2-Chloroaniline) for Corrosion Control of Mild Steel in Acidic Medium." *J. Bio-and Tribo-Corros.*, **6** 1–14 (2020). <https://doi.org/10.1007/s40735-020-00351-0>
20. Bashir, S, Thakur, A, Lgaz, H, Chung, I-M, Kumar, A, "Computational and Experimental Studies on Phenylephrine as Anti-Corrosion Substance of Mild Steel in Acidic Medium." *J. Mol. Liq.*, **293** 111539 (2019). <https://doi.org/10.1016/j.molliq.2019.111539>
21. El Ashry, ESH, El Nemr, A, Esawy, SA, Ragab, S, "Corrosion Inhibitors-Part II: Quantum Chemical Studies on the Corrosion Inhibitions of Steel in Acidic Medium by Some Triazole, Oxadiazole and Thiadiazole Derivatives." *Electrochim. Acta*, **51** 3957–3968 (2006). <https://doi.org/10.1016/j.electacta.2005.11.010>
22. El-Salam, HMA, El-Hafez, GMA, Askalany, HG, Fekry, AM, "A Creation of Poly(N-2-Hydroxyethylaniline-co-2-Chloroaniline) for Corrosion Control of Mild Steel in Acidic Medium." *J. Bio- and Tribo-Corros.*, **6** 53 (2020). <https://doi.org/10.1007/s40735-020-00351-0>
23. Khalaf, MM, Abd El-Lateef, HM, "Corrosion Protection of Mild Steel by Coating with TiO₂ Thin Films Co-Doped with NiO and ZrO₂ in Acidic Chloride Environments." *Mater. Chem. Phys.*, **177** 250–265 (2016). <https://doi.org/10.1016/j.matchemphys.2016.04.026>
24. Abdrabo, WS, Elgandy, B, Soliman, KA, Abd El-Lateef, HM, Tantawy, AH, "Synthesis, Assessment and Corrosion Protection Investigations of Some Novel Peptidomimetic Cationic Surfactants: Empirical and Theoretical Insights." *J. Mol. Liq.*, **315** 113672 (2020). <https://doi.org/10.1016/j.molliq.2020.113672>
25. Khalaf, MM, Tantawy, AH, Soliman, KA, Abd El-Lateef, HM, "Cationic Gemini-Surfactants Based on Waste Cooking Oil as New 'Green' Inhibitors for N80-Steel Corrosion in Sulphuric Acid: A Combined Empirical and Theoretical Approaches." *J. Mol. Struct.*, **1203** 127442 (2020). <https://doi.org/10.1016/j.molstruc.2019.127442>
26. Aly, KI, Mohamed, MG, Younis, O, Mahross, MH, Abdel-Hakim, M, Sayed, MM, "Salicylaldehyde Azine-Functionalized Polybenzoxazine: Synthesis, Characterization, and Its Nanocomposites as Coatings for Inhibiting the Mild Steel Corrosion." *Prog. Org. Coat.*, **138** 105385 (2020). <https://doi.org/10.1016/j.porgcoat.2019.105385>
27. Chafiq, M, Chaoui, A, Lgaz, H, Salghi, R, Bhaskar, KV, Marzouki, R, Bhat, KS, Ali, IH, Khan, MI, Chung, I-M, "Inhibition Performances of Spirocyclopropane Derivatives for Mild Steel Protection in HCl." *Mater. Chem. Phys.*, **243** 122582 (2020). <https://doi.org/10.1016/j.matchemphys.2019.122582>
28. Srivastava, V, Singh, MJJOAE, "Corrosion Inhibition of Mild Steel in Acidic Medium by Poly (Aniline-co-o-Toluidine) Doped with p-Toluene Sulphonic Acid." *J. Appl. Electrochem.*, **40** 2135–2143 (2010)
29. Ashassi-Sorkhabi, H, Ghalebsaz-Jeddi, N, Hashemzadeh, F, Jahani, H, "Corrosion Inhibition of Carbon Steel in Hydrochloric Acid by Some Polyethylene Glycols." *Electrochim. Acta*, **51** 3848–3854 (2006). <https://doi.org/10.1016/j.electacta.2005.11.002>
30. Diggle, J, Downie, T, Goulding, C, "The Dissolution of Porous Oxide Films on Aluminium." *Electrochim. Acta*, **15** 1079–1093 (1970). [https://doi.org/10.1016/0013-4686\(70\)85002-2](https://doi.org/10.1016/0013-4686(70)85002-2)
31. El-Rabieci, MM, Abd El-Aafez, GM, Gaber, AF, Farag, ZR, "Part I. Electropolymerization and Characterization of

- Polymer Coatings on Pt –Electrode.” *Revista de Chimie*, (in progress)
32. Kelen, T, Tüdös, F, “Analysis of the Linear Methods for Determining Copolymerization Reactivity Ratios. I. A New Improved Linear Graphic Method.” *J. Macromol. Sci. A*, **9** 1–27 (1975)
33. Ismail, KM, El-Moneim, AA, Badawy, WA, “Stability of Sputter-Deposited Amorphous Mn-Ta Alloys in Chloride-Free and Chloride-Containing H₂SO₄ Solutions.” *J. Electrochem. Soc.*, **148** C81–C87 (2001)
34. Huang, R, Han, Y, “The Effect of SMAT-Induced Grain Refinement and Dislocations on the Corrosion Behavior of Ti–25Nb–3Mo–3Zr–2Sn Alloy.” *Mater. Sci. Eng. C*, **33** 2353–2359 (2013). <https://doi.org/10.1016/j.msec.2013.01.068>
35. Damaskin, BB, Petrii, OA, Batrakov, VV, *Adsorption of Organic Compounds on Electrodes*. Plenum, New York (1971)

Publisher’s Note Springer Nature remains neutral with regard to jurisdictional claims in published maps and institutional affiliations.